

Quantum Projector Method on Curved Manifolds

V. Melik-Alaverdian,¹ G. Ortiz,² and N. E. Bonesteel³

Received December 22, 1999; revised January 29, 2001

A generalized stochastic method for projecting out the ground state of the quantum many-body Schrödinger equation on curved manifolds is introduced. This random-walk method is of wide applicability to any second order differential equation (first order in time), in any spatial dimension. The technique reduces to determining the proper “quantum corrections” for the Euclidean short-time propagator that is used to build up their path-integral Monte Carlo solutions. For particles with Fermi statistics the “Fixed-Phase” constraint (which amounts to fixing the phase of the many-body state) allows one to obtain stable, albeit approximate, solutions with a variational property. We illustrate the method by applying it to the problem of an electron moving on the surface of a sphere in the presence of a Dirac magnetic monopole.

KEY WORDS: Stochastic or statistical methods; quantum Monte Carlo; fermion methods; generalized diffusion equation; quantum hell physics.

I. INTRODUCTION

The correlated motion of interacting quantum particles gives rise to a wide variety of physical phenomena at different length and time scales, spanning disciplines like chemistry, condensed matter, nuclear, and high energy physics. Novel complex structures can emerge as a consequence of the competing multiple-length scales in the problem. Nonetheless, only a reduced set of interacting problems admits exact closed form solutions⁽¹⁾ and the use of numerical techniques becomes essential if one is looking for accurate solutions not subjected to uncontrolled approximations. Among those techniques, the statistical methods⁽²⁾ offer the potential to study

¹ Department of Physics, University of Rhode Island, Kingston, Rhode Island 02881.

² Theoretical Division, Los Alamos National Laboratory, P.O. Box 1663, Los Alamos, New Mexico 87545.

³ National High Magnetic Field Laboratory and Department of Physics, Florida State University, Tallahassee, Florida 32306-4005.

systems with large number of degrees of freedom, reducing the computational complexity from exponential to polynomial growth. Unfortunately, for fermions (i.e., quantum particles obeying Fermi statistics) the sign problem plagues all useful stochastic algorithms and causes the variance of computed results to increase exponentially with increasing number of fermions.⁽³⁾

The growing interest in physical systems whose state functions are defined on a general metric space makes the quantum mechanics of interacting particles in curved manifolds no longer a mere intellectual exercise, but one with very practical consequences. Perhaps the most well-known examples can be found in cosmology (e.g., matter in strong gravitational fields, atomic spectroscopy as probe of space-time curvature⁽⁴⁾), but the subject is certainly not exclusive to this field. In condensed matter a very elementary case is provided by a deformed crystal. Less well-known ones are mesoscopic graphitic microtubules and fullerenes. All these physical systems are ubiquitous in nature and the crucial role the curvature of the manifold plays has been confirmed by experimental observations (e.g. spectrum of collective excitations⁽⁵⁾). Therefore, the development of stable quantum methods with polynomial complexity in Riemannian manifolds represents a real challenge for many-body theorists.

The present manuscript deals with the (non-relativistic) many-particle Schrödinger equation (SE) in a general metric space and its solution using stochastic techniques. The projector (zero temperature) method we will introduce uses random-walks⁽⁶⁾ to solve this general multidimensional partial differential equation, second order in space coordinates and first order in time. The method is not limited to systems on curved manifolds.⁽⁷⁾ Indeed, it can be applied to a wide variety of inhomogeneous systems (e.g., inhomogeneous semiconductors with a position dependent effective mass). The reason for this, as discussed in Section III, is that the quantum corrections to the Green's function (GF) can be interpreted as being due to those terms which appear in the generalized diffusion equation describing the system once each of the derivatives in that equation have been commuted all the way to the left of each term. This definition of quantum corrections is quite general and can be applied to *any* differential equation which is second order in space and first order in time, regardless of the number of dimensions or any spatial inhomogeneity in the system.

In Section II we present the formulation of the general problem of fermions in curved manifolds. For illustration purposes we develop the formalism for spin- $\frac{1}{2}$ particles in the presence of an external electromagnetic potential. Then, we show how to project out the lowest energy state of a given symmetry in a manifold with curvature, and discuss the resulting Fokker-Planck equations for various distribution functions. In Section III

we derived the relevant propagator and give an interpretation of the emergent “quantum corrections” in the Euclidean action. The path-integral solutions are evaluated using Monte Carlo techniques in Section IV. There, we provide a practical algorithm which emphasizes the changes (with respect to the standard Diffusion Monte Carlo (DMC) technique) due to the metric of the manifold. In Section V we apply such computational implementation to the problem of an electron moving on the surface of a sphere in the presence of a Dirac monopole. Finally, Section VI summarizes the main findings.

II. FERMIONS ON RIEMANNIAN MANIFOLDS

Notation. Consider a differentiable manifold \mathcal{M} of dimension d (e.g., for the two-sphere S^2 , $d=2$) with coordinates $\mathbf{r}_i = (x_i^1, \dots, x_i^d)$ defined on it. If \mathcal{M} is a Riemannian manifold, then it is a metric space, with metric tensor $g^{\mu\nu}(\mathbf{r}_i) = g^{\mu\nu}(i)$ ($\mu, \nu = 1, \dots, d$), such that the distance ds between two points in \mathcal{M} is $ds^2 = g_{\mu\nu}(i) dx_i^\mu dx_i^\nu$ in the usual way.⁽⁹⁾ The metric tensor is positive definite and symmetric $g^{\mu\nu} = g^{\nu\mu}$ (as we will see, this condition is important to define a probability density distribution), and is a function of the coordinates \mathbf{r}_i with the property $g_{\mu\nu}g^{\gamma\nu} = \delta_\mu^\gamma$. Let us consider the coordinate transformation $h: x_i^\mu = h^\mu(x_i^1, \dots, x_i^d)$. Then, a generic second order contravariant ($T^{\mu\nu}$) and covariant tensor ($T_{\mu\nu}$) transform as

$$T^{\mu\nu} = \frac{\partial x_i^\mu}{\partial x_i'^\alpha} \frac{\partial x_i^\nu}{\partial x_i'^\beta} T'^{\alpha\beta}, \quad T_{\mu\nu} = \frac{\partial x_i'^\alpha}{\partial x_i^\mu} \frac{\partial x_i'^\beta}{\partial x_i^\nu} T'_{\alpha\beta}, \quad (1)$$

respectively. Throughout the paper Einstein’s summation convention is assumed.

Formulation of the problem. In this article we will be concerned with finite interacting fermion systems in the presence of an external electromagnetic potential $a_\mu(\mathbf{r}_i) = a_\mu(i) = (\mathbf{A}(i), \phi(i) = 0)$ ($\mathbf{B} = \nabla \wedge \mathbf{A}$ represents a uniform field, \mathbf{A} and ϕ are the vector and scalar potentials, respectively) whose quantum Hamiltonian⁽¹⁰⁾ for motion on the manifold, in the coordinate representation, is given by $\hat{\mathbb{H}} = \hat{\mathbb{H}}_0 + \hat{V}(\{\mathbf{r}_i\}, \{s_i\})$ with

$$\begin{aligned} \hat{\mathbb{H}}_0 = & -D\Delta + i \frac{e\hbar}{2m^*c} \sum_{i=1}^N [2a^\mu(i) \partial_\mu + g^{-1/2}(i) \partial_\mu (g^{1/2}(i) a^\mu(i))] \\ & + \frac{e^2}{2m^*c^2} \sum_{i=1}^N a^\mu(i) a_\mu(i), \end{aligned} \quad (2)$$

$\partial_\mu = \partial/\partial x_i^\mu$, $\Delta = \sum_{i=1}^N \Delta(i)$, where $\Delta = g^{-1/2} \partial_\mu (g^{\mu\nu} g^{1/2} \partial_\nu)$ is the covariant Laplace–Beltrami operator and \hat{V} is a potential energy operator. Notice

that we use the conventional notation where the transformation between different forms of a given tensor is achieved by using the metric tensor (e.g., $a^\mu = g^{\mu\nu} a_\nu$, $a_\mu = g_{\mu\nu} a^\nu$), and $g^{1/2} = \sqrt{\det g_{\mu\nu}}$. This Hamiltonian characterizes the dynamics of N non-relativistic indistinguishable particles of mass m^* , charge e and spin $s_i = \frac{1}{2}$ in a curved space with metric tensor $g^{\mu\nu}$, and $D = \hbar^2/2m^*$. We have assumed that $\hat{\mathbb{H}}$ in curved space has the same form as in flat space (this amounts to a particular operator ordering prescription.)

Given the previous ordering, one can rewrite the Hamiltonian above in terms of the generalized (hermitian) canonical momentum $\mathbf{p}_\mu = -i\hbar(\partial_\mu + \frac{1}{2}\partial_\mu(\ln g^{1/2}))$

$$\hat{\mathbb{H}} = \frac{1}{2m^*} \sum_{i=1}^N g^{-1/4}(i) \Pi_\mu g^{1/2}(i) g^{\mu\nu}(i) \Pi_\nu g^{-1/4}(i) + \hat{V}(\{\mathbf{r}_i\}, \{s_i\}), \quad (3)$$

where the kinetic momentum $\Pi_\mu = \mathbf{p}_\mu - \frac{e}{c} a_\mu$. The first term in Eq. 3 represents the kinetic energy of the system and is the non-relativistic approximation to the Dirac operator. \hat{V} includes the sum of one and two-body local interaction terms (and background potential in the case of a charge neutral system) and Zeeman contribution. The potentials are assumed to be finite almost everywhere and can only be singular at coincident points ($\mathbf{r}_i = \mathbf{r}_j$, $\forall i \neq j$)

We are interested in the stationary solutions of the resulting multidimensional SE

$$i\hbar \partial_i |\Psi\rangle = \hat{\mathbb{H}} |\Psi\rangle, \quad (4)$$

and will restrict ourselves to Hamiltonians which are time-translation invariant. In the usual space-spin formalism the N -fermion states characterizing the system, $\langle X | \Psi \rangle = \Psi(X)$, and all its first derivatives belong to the Hilbert space of antisymmetric (with respect to identical particle (\mathbf{r}_i, s_i)-exchanges) square-integrable functions $\mathcal{H}_N = \mathcal{L}^2(\mathcal{M}^N) \otimes \mathbb{C}^{2^N}$, defined as

$$\mathcal{H}_N = \{\Psi \mid \hat{P}_{ij}\Psi = -\Psi, \text{ and } \|\Psi\| = \sqrt{\langle \Psi | \Psi \rangle} < \infty\}, \quad (5)$$

where $X = (\mathcal{R}, \Sigma)$ ($\mathcal{R} = (\mathbf{r}_1, \dots, \mathbf{r}_N)$ and $\Sigma = (\sigma_1, \dots, \sigma_N)$ are discrete spin variables) and \hat{P}_{ij} represents the permutation of the pairs (\mathbf{r}_i, σ_i) and (\mathbf{r}_j, σ_j) .⁽¹¹⁾

Since the system Hamiltonian can be written as $\hat{\mathbb{H}} = \hat{\mathbb{H}}_{\mathcal{R}}(\mathcal{R}) + \hat{\mathbb{H}}_{\Sigma}(\Sigma)$, the last term representing the Zeeman coupling, the many-body wave function $\Psi(\mathcal{R}, \Sigma)$ can be expressed as a tensor product of a coordinate and a spin function (or a linear combination of such products), $\Psi(\mathcal{R}, \Sigma) = \Phi(\mathcal{R}) \otimes \Xi(\Sigma)$. We want to construct N -fermion eigenstates of $\hat{\mathbb{H}}$, Ψ , that

are also eigenfunctions of the total spin S^2 ($S^2 \Psi(X) = \hbar^2 s(s+1) \Psi(X)$), such that $S = \sum_{i=1}^N s_i$, and this is always possible since $[\hat{\mathbb{H}}, S^2] = 0$. Thus, the configuration part $\Phi(\mathcal{R})$ must have the right symmetry in order to account for the Pauli principle. It turns out that a coordinate state $\Phi(\mathbf{r}_1, \dots, \mathbf{r}_k, \mathbf{r}_{k+1}, \dots, \mathbf{r}_N)$ which is symmetrized according to the Young scheme⁽¹²⁾ and has total spin $s = \frac{N}{2} - k$ will be antisymmetric in the variables $\mathbf{r}_1, \dots, \mathbf{r}_k$, and antisymmetric in the variables $\mathbf{r}_{k+1}, \dots, \mathbf{r}_N$.

Quantum Projection on Curved Manifolds. For a given total spin s we are thus left with the task of solving the stationary many-body SE, $\hat{\mathbb{H}}_{\mathcal{R}} \Phi(\mathcal{R}) = E \Phi(\mathcal{R})$, where $\Phi(\mathcal{R}) = \langle \mathcal{R} | \Phi \rangle$ satisfies the symmetry constraint discussed above. In particular, we are interested in the zero temperature properties of this quantum system, i.e., its ground state (GS) properties. To this end, we study the Euclidean time evolution of the state Φ , i.e., we analytically continue Eq. 4 to imaginary time (Wick rotation, $t \rightarrow -it\hbar$)

$$-\partial_t \Phi = [\hat{\mathbb{H}}_{\mathcal{R}} - E_T] \Phi, \quad (6)$$

whose formal solution $\Phi(t) = \hat{\mathcal{U}}(t) \Phi_T = \exp[-t(\hat{\mathbb{H}}_{\mathcal{R}} - E_T)] \Phi_T$ is used to determine the limiting distribution

$$\Phi_0 \propto \lim_{t \rightarrow \infty} \Phi(t), \quad (7)$$

which is the largest eigenvalue solution of the evolution operator $\hat{\mathcal{U}}(t)$ compatible with the condition $\langle \Phi_0 | \Phi_T \rangle \neq 0$, where Φ_T is a parent state and E_T is a suitable (constant) energy that shifts the zero of the spectrum of $\hat{\mathbb{H}}_{\mathcal{R}}$.

We would like to solve the multidimensional differential equation Eq. 6 using initial value random walks. In this way, starting with an initial population of walkers (whose state space is \mathcal{M}^N) distributed according to $p(\mathcal{R}, t=0) = \Phi_T$ (Φ_T must be positive semi-definite), the ensemble is evolved by successive applications of the short (imaginary) time propagator $\hat{\mathcal{U}}(\tau)$ ($\tau = t/M$, and M is the number of time slices) to obtain the limiting distribution Φ_0 . Then, we can introduce a ‘‘pseudo partition function’’

$$\mathcal{Z} = \langle \Phi_T | \hat{\mathcal{U}}(t) \Phi_T \rangle \quad (8)$$

in terms of which we can determine the GS energy E_0 as

$$E_0 - E_T = \lim_{t \rightarrow \infty} -\frac{1}{t} \ln \mathcal{Z}. \quad (9)$$

Similarly, other GS expectation values, e.g., $\langle \Phi_0 | \hat{\mathcal{O}} \Phi_0 \rangle$, can be obtained as derivatives (with respect to a coupling constant J) of a modified pseudo

partition function \mathcal{Z}_J whose evolution operator has a modified Hamiltonian, $\hat{\mathbb{H}}_{\mathcal{R}} + J\hat{\mathcal{O}}$.

In order to reduce statistical fluctuations in the measured quantities (i.e., observables) one can guide the random walk with an approximate wave function, Φ_G , which contains as much of the essential physics as possible (including cusp conditions at possible singularities of the potential \hat{V}). Then, instead of sampling the wave function $\Phi(t)$ one samples the distribution $\tilde{f}(\mathcal{R}, t) = \Phi(t) \Phi_G$ (properly normalized) with the initial time condition $\tilde{f}(\mathcal{R}, t=0) = \Phi_T \Phi_G$. Expectation values of operators $\hat{\mathcal{O}}$ (observables) that commute with the Hamiltonian have a particularly simple form for guided walkers. For instance,

$$\lim_{t \rightarrow \infty} \frac{\langle \Phi_T | \hat{\mathcal{O}} \hat{\mathcal{U}}(t) \Phi_T \rangle}{\langle \Phi_T | \hat{\mathcal{U}}(t) \Phi_T \rangle} = \langle \Phi_G^{-1} \hat{\mathcal{O}} \Phi_T \rangle_{\tilde{f}(t \rightarrow \infty)}, \quad (10)$$

where the average $\langle \mathcal{A} \rangle_{\tilde{f}}$ stands for

$$\langle \mathcal{A} \rangle_{\tilde{f}} = \frac{\int_{\mathcal{M}^N} \omega \tilde{f}(\mathcal{R}, t \rightarrow \infty) \mathcal{A}(\mathcal{R})}{\int_{\mathcal{M}^N} \omega \tilde{f}(\mathcal{R}, t \rightarrow \infty)}, \quad (11)$$

$\tilde{f}(\mathcal{R}, t \rightarrow \infty)$ is the long-time stationary probability of the system, and the (invariant) volume element ω is given by the dN -form⁽¹³⁾

$$\omega = \left[\prod_{i=1}^N g^{1/2}(i) \right] dx_1^1 \wedge \cdots dx_1^d \wedge \cdots dx_N^d. \quad (12)$$

It is important to stress that Φ_T and the guiding function Φ_G can, in principle, be different functions, although most of the practical calculations use the same function. It turns out that this importance sampling procedure is decisive to get sensible results when the potential \hat{V} presents some singularities.

Notice, however, that the quantum Hamiltonian $\hat{\mathbb{H}}$ breaks explicitly time-reversal symmetry, meaning that in general Φ will be a complex-valued function. Even if Φ were real-valued, because it represents a fermion wave function it can acquire positive and negative values (the case where $\mathcal{E}(\mathcal{Z})$ is totally antisymmetric being the exception). Then, it is clear that we cannot in principle interpret Φ or \tilde{f} as a probability density.

For reasons that will become clear later⁽¹⁴⁾ we will be interested in sampling the probability density $\bar{f}(\mathcal{R}, t) = |\tilde{f}(\mathcal{R}, t)|$. The generalized diffusion equation in curved space for the importance-sampled function \bar{f} can be derived directly from Eq. 6 with the result

$$\partial_t \bar{f} = D \sum_{i=1}^N [g^{-1/2}(i) \partial_\mu (g^{\mu\nu}(i) g^{1/2}(i) (\partial_\nu \bar{f} - \bar{f} F_\nu))] - (E_L - E_T) \bar{f}, \quad (13)$$

where the drift velocity $F_v(\mathcal{R}) = \partial_v \ln \Phi_G^2$, and the “local energy” of the effective (“Fixed-Phase”) Hamiltonian \hat{H}_{FP} is $E_L(\mathcal{R}) = \Phi_G^{-1} \hat{H}_{FP} \Phi_G$ with

$$\hat{H}_{FP} = -D\Delta + D \sum_{i=1}^N \left[(\partial^\mu \chi(\mathcal{R}) - \frac{e}{\hbar c} a^\mu(i)) (\partial_\mu \chi(\mathcal{R}) - \frac{e}{\hbar c} a_\mu(i)) \right] + \hat{V}(\mathcal{R}), \quad (14)$$

where $\chi(\mathcal{R})$ is the phase of the many-body state Φ , i.e., $\Phi = |\Phi| \exp[i\chi]$.⁽¹⁵⁾ The differential equation satisfied by the distribution function \bar{f} is formally equivalent to the one describing Brownian motion on a general manifold (including generation and recombination processes), and corresponds to a Kramers-Moyal expansion with exactly two terms. In fact, we can rewrite the equation above as a Fokker-Planck equation for dN continuous stochastic variables $\{\mathbf{r}_i\}_{i=1, \dots, N}$

$$\partial_t \bar{f} = \{ \bar{\mathcal{L}}_{FP} - (\bar{E}_L - E_T) \} \bar{f}, \quad (15)$$

where the (time-independent) Fokker-Planck operator $\bar{\mathcal{L}}_{FP}$ is given by

$$\bar{\mathcal{L}}_{FP} \bullet = \sum_{i=1}^N [\partial_\mu \partial_\nu (\bar{D}^{\mu\nu}(i) \bullet) - \partial_\mu (\bar{D}^\mu(\mathcal{R}) \bullet)]. \quad (16)$$

The diffusion matrix (contravariant tensor) $\bar{D}^{\mu\nu}$ and drift \bar{D}^μ (which does not transform as a contravariant vector) are given by

$$\bar{D}^{\mu\nu} = Dg^{\mu\nu} \quad (17)$$

$$\bar{D}^\mu = \bar{D}^{\mu\nu} F_\nu + \partial_\nu \bar{D}^{\mu\nu} - \bar{D}^{\mu\nu} \Gamma_{\nu\sigma}^\sigma, \quad (18)$$

where $\Gamma_{\mu\nu}^\sigma$ is the Christoffel symbol of the second kind

$$\Gamma_{\mu\nu}^\sigma = \frac{1}{2} g^{\sigma\rho} (\partial_\mu g_{\nu\rho} + \partial_\nu g_{\mu\rho} - \partial_\rho g_{\mu\nu}) \quad (19)$$

$$\Gamma_{\nu\sigma}^\sigma = \frac{1}{2} \partial_\nu \ln g, \quad (20)$$

and the modified local energy

$$\bar{E}_L = E_L + \bar{D}^{\mu\nu} \Gamma_{\mu\sigma}^\sigma F_\nu + \partial_\mu (\bar{D}^{\mu\nu} \Gamma_{\nu\sigma}^\sigma). \quad (21)$$

Notice, however, that singularities in the “quantum corrections”⁽¹⁶⁾ to the local energy E_L due to the metric, can induce very large fluctuations in \bar{E}_L . Moreover, the probability density \bar{f} does not transform as a scalar function ($\bar{f}(\mathcal{R}, t) \bar{\omega} = \bar{f}(\mathcal{R}', t) \bar{\omega}'$, where the primes represent the transformed coordinates and $\bar{\omega} = dx_1^1 \wedge \dots \wedge dx_1^d \wedge \dots \wedge dx_N^d$ is a volume element in \mathcal{M}^N).

Therefore, it is more convenient to work with a probability density that is a scalar

$$f(\mathcal{R}, t) = \left[\prod_{i=1}^N g^{1/2}(i) \right] \bar{f}(\mathcal{R}, t). \quad (22)$$

The differential equation f satisfies is of the form Eq. 15 with bar quantities replaced by unbar ones (e.g. $\bar{\mathcal{L}}_{\text{FP}} \rightarrow \mathcal{L}_{\text{FP}}$). It turns out that $D^{\mu\nu} = \bar{D}^{\mu\nu}$ and the drift (which is not a tensor)

$$D^\mu = D^{\mu\nu} F_\nu + \partial_\nu D^{\mu\nu} + D^{\mu\nu} \Gamma_{\nu\sigma}^\sigma. \quad (23)$$

Note that in this case the quantum correction to the local energy vanishes. Furthermore, if the metric is diagonal, i.e., $g_{\mu\nu} = g^{1/2} \delta_{\mu\nu}$, then the correction to the flat space drift also vanishes, i.e., $\partial_\nu D^{\mu\nu} + D^{\mu\nu} \Gamma_{\nu\sigma}^\sigma = 0$, and $D^\mu = Dg^{-1/2} F^\mu$. This last remark is quite important, specially for $d = 2$ where it is *always* possible to choose a coordinate system ($\mathbf{r}_i = (\xi_i^1, \xi_i^2)$) where the metric tensor is diagonal (conformal gauge⁽¹⁷⁾), and use the conformal parameterization ($z_i = \xi_i^1 + i\xi_i^2$, $\bar{z}_i = \xi_i^1 - i\xi_i^2$) which greatly simplifies the resulting expressions (see Section V).

III. DERIVATION OF GREEN'S FUNCTION

The generalized Fokker–Planck Eq. 15 describes the time evolution of a distribution function f which is completely determined by the distribution function at $t = t_0 = 0$. In this sense it describes a continuous stochastic process that is Markovian. Because it represents a Markov process, the conditional probability that if the system configuration is \mathcal{R} at time $t = 0$ it will jump to \mathcal{R}' in time t (importance-sampled GF) $G(\mathcal{R} \rightarrow \mathcal{R}'; t)$ contains all information about the process, and the probability densities $f(\mathcal{R}, t + \tau)$ and $f(\mathcal{R}, t)$ are connected by

$$f(\mathcal{R}', t + \tau) = \int_{\mathcal{A}^N} \omega G(\mathcal{R} \rightarrow \mathcal{R}'; \tau) f(\mathcal{R}, t), \quad (24)$$

where the transition probability $G(\mathcal{R} \rightarrow \mathcal{R}'; \tau)$ is formally given by

$$G(\mathcal{R} \rightarrow \mathcal{R}'; \tau) = \tilde{\Phi}_G(\mathcal{R}') \langle \mathcal{R}' | \exp[-\tau(\hat{H}_{\text{FP}} - E_T)] | \mathcal{R} \rangle \tilde{\Phi}_G^{-1}(\mathcal{R}), \quad (25)$$

with

$$\tilde{\Phi}_G(\mathcal{R}) = \left[\prod_{i=1}^N g^{1/2}(\mathbf{r}_i) \right] \Phi_G(\mathcal{R}), \quad (26)$$

and boundary condition $G(\mathcal{R} \rightarrow \mathcal{R}'; 0) = [\prod_{i=1}^N g^{-1/2}(i)] \delta(\mathcal{R} - \mathcal{R}')$.

Iteration of (24) allows one to express the evolution of $f(\mathcal{R}', t)$ from the initial distribution $f(\mathcal{R}, t = 0)$ in terms of the short-time GF as

$$f(\mathcal{R}', t) = \int_{\mathcal{M}^N} \omega_{M-1} \cdots \int_{\mathcal{M}^N} \omega_0 G(\mathcal{R}_{M-1} \rightarrow \mathcal{R}_M; \tau) \cdots G(\mathcal{R}_0 \rightarrow \mathcal{R}_1; \tau) f(\mathcal{R}_0, 0), \quad (27)$$

where $t = M\tau$; $\mathcal{R}_0 = \mathcal{R}$ and $\mathcal{R}_M = \mathcal{R}'$. To use (27) as the basis of a numerical simulation we require an expression for the short-time GF which, to $\mathcal{O}(\tau^2)$, is given by

$$G(\mathcal{R} \rightarrow \mathcal{R}'; \tau) = G_b(\mathcal{R} \rightarrow \mathcal{R}'; \tau) \prod_{i=1}^N G_i^0(\mathcal{R} \rightarrow \mathcal{R}'; \tau) \quad (28)$$

where

$$G_b(\mathcal{R} \rightarrow \mathcal{R}'; \tau) = \exp \left[-\tau \left(\frac{[E_L(\mathcal{R}) + E_L(\mathcal{R}')] }{2} - E_T \right) \right], \quad (29)$$

is the short-time GF associated with the local energy term in (15) and $G_i^0(\mathcal{R} \rightarrow \mathcal{R}'; \tau)$ is the GF for the i th particle associated with the generalized drift and diffusion terms. The form of this GF can be obtained by solving the following differential equation corresponding to the diffusion of a single particle

$$\partial_\mu \partial_\nu (D^{\mu\nu}(\mathbf{r}) G^0(\mathbf{r}, \tau)) - \partial_\mu (D^\mu(\mathbf{r}) G^0(\mathbf{r}, \tau)) = \partial_\tau G^0(\mathbf{r}, \tau), \quad (30)$$

subject to the boundary condition $G^0(\mathbf{r}, \tau = 0) = g^{-1/2}(\mathbf{r}) \delta^d(\mathbf{r})$ indicating that, for what follows, the prepoint is the origin $\mathbf{0}$.

It is, of course, possible to treat (30) as a generalized diffusion equation on a flat space in which the diffusion ‘constant’ $D^{\mu\nu}(\mathbf{r})$ and the drift velocity $D^\mu(\mathbf{r})$ depend on position. One can then introduce the usual flat-space Fourier transform of the GF

$$\tilde{G}^0(\mathbf{k}, \tau) = \int d^d \mathbf{r} G^0(\mathbf{r}, \tau) e^{i\mathbf{k} \cdot \mathbf{r}}, \quad (31)$$

which satisfies the equation

$$\frac{1}{(2\pi)^d} \int d^d \mathbf{k}' (-k_\mu k_\nu \tilde{D}^{\mu\nu}(\mathbf{k}') + ik_\mu \tilde{D}^\mu(\mathbf{k}')) \tilde{G}^0(\mathbf{k} - \mathbf{k}', \tau) = \partial_\tau \tilde{G}^0(\mathbf{k}, \tau) \quad (32)$$

with boundary condition $\tilde{G}^0(\mathbf{k}, \tau = 0) = g^{-1/2}(\mathbf{0})$, (all Fourier transformed functions are indicated by tildes). Because $\tilde{G}^0(\mathbf{k}, \tau)$ is independent of \mathbf{k} at $\tau = 0$, for short times τ

$$\tilde{G}^0(\mathbf{k}', \tau) = \tilde{G}^0(\mathbf{k}, \tau) + \mathcal{O}(\tau). \quad (33)$$

Substituting (33) into (32) and performing the \mathbf{k}' integration then gives

$$(-k_\mu k_\nu D^{\mu\nu}(\mathbf{0}) + ik_\mu D^\mu(\mathbf{0})) \tilde{G}^0(\mathbf{k}, \tau) + \mathcal{O}(\tau) = \partial_\tau \tilde{G}^0(\mathbf{k}, \tau), \quad (34)$$

which, upon Fourier transforming back to real space, yields

$$D^{\mu\nu}(\mathbf{0}) \partial_\mu \partial_\nu G^0(\mathbf{r}, \tau) - D^\mu(\mathbf{0}) \partial_\mu G^0(\mathbf{r}, \tau) + \mathcal{O}(\tau) = \partial_\tau G^0(\mathbf{r}, \tau). \quad (35)$$

The space dependent quantities $D^{\mu\nu}$ and D^μ are now constants, evaluated at the origin, i.e., the **prepoint**. The price for this simplification is that the left hand side of (35) is now only accurate to $\mathcal{O}(\tau)$. However, because of the time derivative on the right hand side of (35), this is sufficient to obtain G^0 to the required accuracy of order $\mathcal{O}(\tau^2)$.

Equation (35) now has the form of a standard ‘drift and diffusion’ equation and the GF can be obtained by the usual methods. Using the fact that $D^{\mu\nu} = Dg^{\mu\nu}$ we thus obtain the following expression for $G_i^0(\mathcal{R} \rightarrow \mathcal{R}'; \tau)$,

$$G_i^0(\mathcal{R} \rightarrow \mathcal{R}'; \tau) = \left(\frac{1}{4\pi D\tau} \right)^{d/2} \times \exp \left[- \frac{(x'_i{}^\mu - x_i^\mu - \tau D^\mu(\mathcal{R})) g_{\mu\nu}(\mathbf{r}_i) (x'_i{}^\nu - x_i^\nu - \tau D^\nu(\mathcal{R}))}{4D\tau} \right], \quad (36)$$

that is, a Gaussian distribution with variance matrix $2D^{\mu\nu}(\mathcal{R})$ and mean $x_i^\mu + \tau D^\mu(\mathcal{R})$.

The form of the GF given in (36) is precisely that which is required for performing a numerical simulation of (15). This is because the diffusion and drift velocity are evaluated explicitly at the prepoint. While one might naively think that these quantities could, to sufficient accuracy, just as well be evaluated at the postpoint, x'_i , this is not the case – replacing \mathcal{R} with \mathcal{R}' in either the diffusion or drift velocity leads to unacceptable $\mathcal{O}(\tau)$ corrections to the short-time GF (this GF is not symmetric in the exchange of the arguments \mathcal{R} and \mathcal{R}' since it is not the GF of an Hermitian operator).

IV. COMPUTATIONAL IMPLEMENTATION

In this Section we present an algorithm for computing the GS properties of quantum many-body systems defined on a curved manifold with general metric $g^{\mu\nu}$. Since most parts of the algorithm follow closely the standard DMC method, described for instance in ref. 18, we will simply emphasize their main differences. Figure 1 shows a schematic flow diagram of the algorithm described in this Section.

As mentioned in the Introduction GS expectation values are obtained by averaging over a large number of particle configurations generated according to a certain limiting probability distribution $p(\mathcal{R}, t \rightarrow \infty)$. There is some freedom in the choice of this distribution $p(\mathcal{R}, t)$, however, to reduce statistical fluctuations in the observables to be computed it is more efficient to use the so-called *importance-sampled* distribution $\bar{f}(\mathcal{R}, t)$, which is the product of the absolute value of the solution of the time-dependent SE, $\Phi(\mathcal{R}, t)$, and some positive function $\Phi_G(\mathcal{R})$ that is the best available

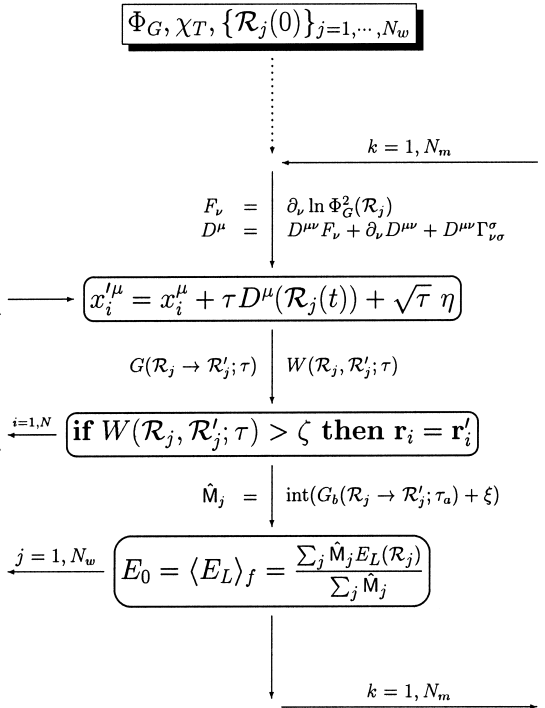


Fig. 1. A schematic of the Fixed-Phase method for curved manifolds with general metric $g^{\mu\nu}$. See the text for notation.

approximation to the modulus of the GS eigenfunction. In a curved manifold, on the other hand, it is more convenient to work with the *modified importance-sampled* distribution $f(\mathcal{R}, t)$, defined as a product of the conventional importance-sampled distribution $\bar{f}(\mathcal{R}, t)$ and the metric (see Eq. 22).

The propagation of particle configurations in time τ is determined by the conditional probability $G(\mathcal{R} \rightarrow \mathcal{R}'; \tau)$, whose separation into a diffusion (plus drift) and branching parts (see Eq. 28) makes it very simple to simulate numerically. The Gaussian term represents propagation according to the equation $x'_i{}^\mu = x_i{}^\mu + \tau D^\mu(\mathcal{R}) + \sqrt{\tau} \eta$, where η is a Gaussian random variable with zero mean and a variance of $2D^{\mu\nu} = 2Dg^{\mu\nu}$. The effect of the term $\tau D^\mu(\mathcal{R})$ is to superimpose a drift velocity on the random diffusion process so that particle configurations are directed towards regions of configuration space where $\Phi_G(\mathcal{R})$ is large. The move from \mathcal{R} to \mathcal{R}' is then accepted with probability $A(\mathcal{R} \rightarrow \mathcal{R}'; \tau) \equiv \min(1, W(\mathcal{R}, \mathcal{R}'; \tau))$, where

$$W(\mathcal{R}, \mathcal{R}'; \tau) \equiv \left[\prod_{i=1}^N \frac{g(\mathbf{r}'_i)}{g(\mathbf{r}_i)} \right] \left| \frac{\Phi_G(\mathcal{R}')}{\Phi_G(\mathcal{R})} \right|^2 \frac{G(\mathcal{R}' \rightarrow \mathcal{R}; \tau)}{G(\mathcal{R} \rightarrow \mathcal{R}'; \tau)}. \quad (37)$$

The branching term $G_b(\mathcal{R} \rightarrow \mathcal{R}'; \tau)$ in Eq. 29, determines the creation and annihilation of configurations (walkers) at the point \mathcal{R}' after a move. If the size of the ensemble of walkers at any time t is defined as $\mathcal{P}(t) = \int_{\mathcal{M}^N} \bar{\omega} f(\mathcal{R}, t)$ then, its rate of change is given by

$$\partial_t \mathcal{P}(t) = - \int_{\mathcal{M}^N} \bar{\omega} [E_L(\mathcal{R}) - E_T] f(\mathcal{R}, t). \quad (38)$$

Therefore, if the local energy $E_L(\mathcal{R})$ is a smooth function of \mathcal{R} , and the trial energy E_T is suitably adjusted, the size of the ensemble of walkers will remain approximately constant as the configurations propagate. In particular, if the local energy is constant and equal to E_T then the fluctuations in the ensemble size will vanish. To ease notation, in the rest of the paper we will only consider the standard situation $\Phi_T = \Phi_G$. In such a case, GS expectation values of a generic observable $\hat{\mathcal{O}}$ will be computed as

$$\begin{aligned} \lim_{t \rightarrow \infty} \frac{\langle \Phi_G | \hat{\mathcal{O}} \hat{\mathcal{U}}(t) \Phi_G \rangle}{\langle \Phi_G | \hat{\mathcal{U}}(t) \Phi_G \rangle} &= \langle \Phi_G^{-1} \hat{\mathcal{O}} \Phi_G \rangle_{f(t \rightarrow \infty)} \\ &= \int_{\mathcal{M}^N} \bar{\omega} \frac{f(\mathcal{R}, t \rightarrow \infty)}{\mathcal{P}(t \rightarrow \infty)} [\Phi_G^{-1} \hat{\mathcal{O}} \Phi_G](\mathcal{R}). \end{aligned} \quad (39)$$

V. EXAMPLE: ELECTRON-MONOPOLE IN S^2

As an example application of the method we have developed in the previous Sections, consider the problem of a single particle of charge e , mass m^* and vector position $\mathbf{r} = (x^1, x^2, x^3)$ in \mathbb{R}^3 confined to the surface of a sphere of radius R centered at the origin ($\mathcal{M} = S^2$, $N = 1$) moving in the presence of the vector potential of a Dirac monopole at the origin. This problem can be solved in closed form and so constitutes an ideal model system for testing the accuracy of the stochastic solutions we can obtain using the formalism developed in previous Sections.

The Pauli Hamiltonian for a spinless particle in S^2 is

$$\hat{\mathbb{H}}_{\mathcal{R}} = \frac{|\hat{\mathbf{f}} \wedge (-i\hbar\nabla - (e/c)\mathbf{A})|^2}{2m^*} = \frac{|\mathbf{L}|^2 - \hbar^2 \mathcal{S}^2}{2m^* R^2}, \quad (40)$$

where $\hat{\mathbf{f}} = \mathbf{r}/R$, and \mathbf{A} is the monopole vector potential ($\nabla \wedge \mathbf{A} = B\hat{\mathbf{f}}$, B being the strength of the radial field). Therefore, the total number of flux quanta $2\mathcal{S}$ piercing the surface of the sphere is given by $2\mathcal{S} = 4\pi R^2 B/\phi_0$, where $\phi_0 = hc/|e|$ is the elementary flux quantum. Following Wu and Yang⁽²⁰⁾ the angular momentum operators are defined as $\mathbf{L} = \mathbf{r} \wedge (-i\hbar\nabla - (e/c)\mathbf{A}) + \hbar\mathcal{S}\hat{\mathbf{f}}$. If we choose a gauge where the vector potential is $\mathbf{A} = -BR \cot \theta \hat{\varphi}$, then the Hamiltonian, Eq. 40, can be written as

$$\hat{\mathbb{H}}_{\mathcal{R}} = \frac{D}{R^2} \left[-\partial_{\theta}^2 - \frac{1}{\sin^2 \theta} \partial_{\varphi}^2 - \cot \theta \partial_{\theta} + 2i\mathcal{S} \frac{\cot \theta}{\sin \theta} \partial_{\varphi} + \mathcal{S}^2 \cot^2 \theta \right], \quad (41)$$

in terms of the usual spherical angles θ and φ ($0 \leq \theta \leq \pi$, $0 \leq \varphi < 2\pi$, see Fig. 2.) The eigenstates of this Hamiltonian are monopole harmonics (normalized to 1)⁽²⁰⁾

$$\begin{aligned} Y_{\mathcal{S}, n, m} &= \mathcal{N}_{\mathcal{S}nm} (-1)^{\mathcal{S}+n-m} \exp[-i\mathcal{S}\varphi] u^{\mathcal{S}+m} v^{\mathcal{S}-m} \mathcal{F}(|u|, |v|), \\ \mathcal{F}(|u|, |v|) &= \sum_{k=0}^n (-1)^k \binom{n}{k} \binom{2\mathcal{S}+n}{\mathcal{S}+n-m-k} (v\bar{v})^{n-k} (u\bar{u})^k, \\ \mathcal{N}_{\mathcal{S}nm} &= \left(\frac{2\mathcal{S}+2n+1}{4\pi} \frac{(\mathcal{S}+n-m)!(\mathcal{S}+n+m)!}{n!(2\mathcal{S}+n)!} \right)^{1/2}, \end{aligned} \quad (42)$$

where $u = \cos(\theta/2) \exp[i\varphi/2]$ and $v = \sin(\theta/2) \exp[-i\varphi/2]$ are spinor coordinates, n is the Landau level quantum number, and $m = -\mathcal{S}-n, -\mathcal{S}-n+1, \dots, \mathcal{S}+n$ is the (L_{x^3}) angular momentum quantum

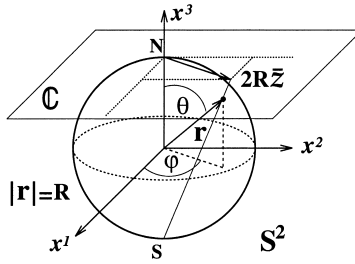


Fig. 2. Spherical and stereographic projection coordinates. R is the radius of the two-sphere S^2 . Notice that points on the sphere are projected onto the complex plane ($z \in \mathbb{C}$) from the southern pole.

number which labels degenerate states within the n^{th} level. In the sum above the binomial coefficient $\binom{\alpha}{\beta}$ vanishes when $\beta > \alpha$ or $\beta < 0$. The energy of a state with Landau level quantum number n is given by

$$E_n = \left(2n + 1 + \frac{n(n+1)}{\mathcal{L}} \right) \frac{\hbar\omega_c}{2}, \quad (43)$$

where ω_c is the cyclotron frequency ($\omega_c = |e| B/m^*c$).

The electron-monopole problem can be reformulated in a way consistent with the notations introduced in the previous Sections. First, instead of the spherical angles θ and φ we introduce new coordinates z and \bar{z} , where $z = \tan(\theta/2) \exp[-i\varphi]$, and \bar{z} is its complex conjugate. Geometrically, this transformation can be viewed as a stereographic projection of the sphere onto the plane, as illustrated in Fig. 2. The Hamiltonian can then be rewritten as

$$\hat{H}_{\mathcal{A}} = \frac{i}{m^*} g^{-1/4} (p_z - \mathcal{A}(z))(p_{\bar{z}} - \bar{\mathcal{A}}(\bar{z})) g^{1/4} + \frac{D\mathcal{L}}{R^2}, \quad (44)$$

in terms of the (non-hermitian) canonical momenta p_z and $p_{\bar{z}}$, and

$$\mathcal{A}(z) = -i \frac{\hbar\mathcal{L}}{2} z \left(\frac{1 - |z|^2}{|z|^2(1 + |z|^2)} \right), \quad (45)$$

with metric tensor

$$g^{\mu\nu}(z, \bar{z}) = \begin{pmatrix} 0 & \frac{(1+z\bar{z})^2}{2R^2} \\ \frac{(1+z\bar{z})^2}{2R^2} & 0 \end{pmatrix}. \tag{46}$$

Notice that the metric tensor is diagonal when written in terms of (ξ^1, ξ^2) , such that $z = \xi^1 + i\xi^2$, i.e., $g^{\mu\nu}(\xi^1, \xi^2) = \frac{(1+|z|^2)^2}{4R^2} \delta^{\mu\nu}$ (i.e, it corresponds to the conformal gauge). The drift is then simply $D_\mu = DF_\mu$.

It is evident that one cannot make a probability density out of a complex and/or antisymmetric wave function. This is the reason why we decided to write down Fokker–Planck equations for the distribution f (or \bar{f}) and not \tilde{f} . Nevertheless, the phase factor associated with the original complex distribution must show up in the evaluation of the expectation values. It is well-known that this causes the variance of the computed results to increase exponentially with increasing number of degrees of freedom. This problem is known as the fermion-phase⁽²¹⁾ catastrophe. To obtain stable, albeit approximate, path-integral solutions whose stochastic determination has a polynomial, instead of exponential, complexity we will use the Fixed-Phase (FP) method.⁽¹⁵⁾

The stochastic method mentioned above allows one to obtain the exact energy eigenvalues of the electron-monopole problem in S^2 iff we know the exact phase of the eigenfunctions. In other words, if the trial state is chosen such that it has the exact GS phase, then independently of its modulus our stochastic approach will lead to the exact GS energy. Similarly, if the trial state has a phase corresponding to an excited state eigenfunction then we will obtain the exact excited state energy eigenvalue. Below we construct simple trial states for the ground and first excited states of the one particle problem. Their modulus are then used as guiding functions Φ_G . Using these trial states we will apply our technique and illustrate the main ideas of our method.

Ground State ($n = 0$). The $2\mathcal{L} + 1$ degenerate GSs of the electron-monopole system are labeled by their L_x angular momentum quantum numbers $m = -\mathcal{L}, \dots, \mathcal{L}$. Here we consider the $m = \mathcal{L}$ GS for which the exact (unnormalized) wave function is

$$\psi_{gs} = \left(\frac{|z|}{z(1+|z|^2)} \right)^{\mathcal{L}} \equiv |\psi_{gs}| e^{i\varphi_{gs}}. \tag{47}$$

Now consider the following two trial states

$$\psi_{T1} = \left(\frac{|z|}{z(1+|z|^2)} \right)^{\mathcal{S}} \frac{1}{1+\lambda|z|^2}, \quad \psi_{T2} = \left(\frac{|z|}{z(1+|z|^2)} \right)^{\mathcal{S}} \left(\frac{|z|}{z} \right)^{\alpha} \quad (48)$$

where λ and α are real valued constants. For $\lambda = 0$ and $\alpha = 0$ these states are both equal to the exact GS, ψ_{gs} . For $\lambda \neq 0$, the modulus of ψ_{T1} is no longer equal to that of the exact GS, but the phase is *exact*, while for $\alpha \neq 0$, the modulus of ψ_{T2} is exact, but the phase is approximate. If ψ_{T1} is used as a trial state in a FP DMC simulation the resulting energy should therefore be the *exact* GS energy $E_0 = \hbar\omega_c/2$, while if ψ_{T2} is used the simulation will not lead to the exact GS energy, but instead yield a variational upper bound.

The trial state used in a FP DMC simulation should be constructed to be the *best available* approximation to the exact eigenstate. For example, since the modulus of ψ_{T2} is exact, the drift velocity F will also be exact and, in the absence of the branching term, will lead to the exact density distribution. It is straightforward to show that $F_{\mu} = \partial_{z^{\mu}} \ln |\psi_{T2}|^2$ is given by

$$F_1 = -\frac{4\mathcal{S}\xi^1}{1+|z|^2}, \quad F_2 = -\frac{4\mathcal{S}\xi^2}{1+|z|^2}, \quad (49)$$

indicating that walkers are guided away from regions where the wave function is small. It follows that the particle tends to spend most of its time near the top of the sphere ($\theta = 0$) which leads to a potential problem when we consider the local energy,

$$E_L = |\psi_{T2}|^{-1} \hat{H}_{FP} |\psi_{T2}| = \frac{\hbar\omega_c}{2} \left[1 + \frac{(1+|z|^2)^2}{\mathcal{S}} \left(\frac{\alpha\mathcal{S}}{1+|z|^2} + \frac{\alpha^2}{4|z|^2} \right) \right] \quad (50)$$

which is *not* exact due to the approximate phase of the trial state. In particular, E_L *diverges* as $|z| \rightarrow 0$, and because the drift pushes the particle towards $z = 0$, there will be large fluctuations in the local energy which can lead to huge fluctuations in the population size. Thus, in this particular example, small values for α ($\alpha \ll 1$) must be taken in order to assure fast convergence and good statistical accuracy.

Figure 3 shows the results of FP DMC simulations, using the algorithm developed in this paper, for the difference between computed and exact GS energies using trial state $\psi_{T1}(\lambda = 1)$ (circles) and trial state $\psi_{T2}(\alpha = 0.001)$ (squares) for different values of the time step τ . The $\tau \rightarrow 0$ extrapolated values are also shown.⁽²²⁾ As expected, when ψ_{T1} is used the extrapolated energy agrees within statistical accuracy with the exact result, but when trial state ψ_{T2} is used we obtain a variational upper bound for the exact GS energy.

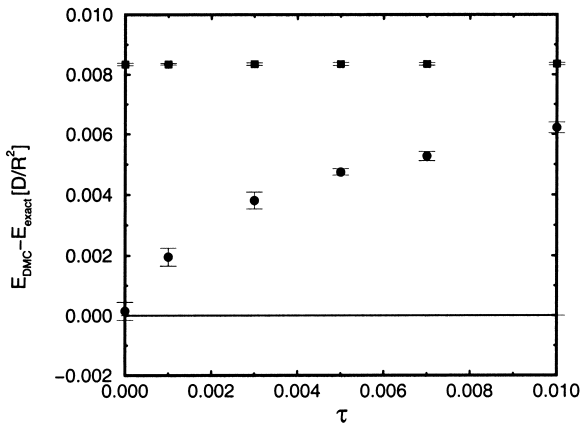


Fig. 3. The difference between computed and exact ground state energies for the trial state with the exact phase $\psi_{T1}(\lambda = 1)$ (circles) and the trial state with an approximate phase $\psi_{T2}(\alpha = 0.001)$ (squares) for various values of time step τ . The $\tau = 0$ extrapolated results are also displayed. Using a trial state with the exact phase in the FP DMC simulations allows one to solve the problem exactly, while using a trial state with an approximate phase allows one to obtain a variational upper bound for the exact solution.

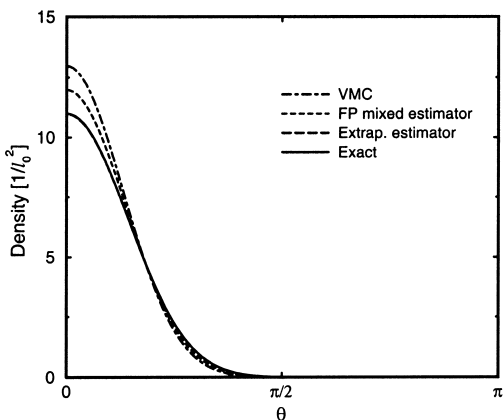


Fig. 4. Ground state density for the exact ground state $\psi_{T1}(\lambda = 0)$ (Exact), the trial state $\psi_{T1}(\lambda = 1)$ (VMC), the density obtained in FP diffusion Monte Carlo with trial state $\psi_{T1}(\lambda = 1)$ at time step $\tau = 0.001$ (FP mixed estimator), and the extrapolated density defined as ratio of the square of FP density to the variational density. The diffusion Monte Carlo density (FP mixed estimator) improves on the variational result but still differs from the exact one. The extrapolated estimator for the density constructed by combining both, the FP mixed estimator and the variational density makes it possible to improve on FP density and is very close to the exact result. The density is normalized in such a way that its integral over the surface of the sphere is $4\pi R^2$. The magnetic length is $l_0 = \sqrt{\hbar c / |e| B}$.

In Fig. 4 the density profiles for the exact GS $\psi_{gs} = \psi_{T1}(\lambda = 0)$ (Exact), the trial state $\psi_{T1}(\lambda = 1)$ (VMC), the density obtained in FP DMC with trial state $\psi_{T1}(\lambda = 1)$ (FP mixed estimator), and the extrapolated density defined as ratio of the square of FP density to the variational density corresponding to $\psi_{T1}(\lambda = 1)$, are shown. Note that since the density in our DMC calculation is determined as a mixed estimate (see Eq. 10), and the density operator does not commute with the Hamiltonian between the DMC solution and the trial state, the corresponding density profile (FP mixed estimator) improves on the variational result but still differs from the exact one. The extrapolated estimator constructed by combining both the FP and variational estimators makes it possible to improve on the FP density, and is seen to be very close to the exact result.

First Excited State ($n = 1$). Consider the first excited state of the electron-monopole system. Taking $m = \mathcal{L} + 1$ the exact wave function is

$$\psi_{es} = \left(\frac{|z|}{z(1+|z|^2)} \right)^{\mathcal{L}+1} |z| = |\psi_{es}| e^{i\varphi_{es}}. \quad (51)$$

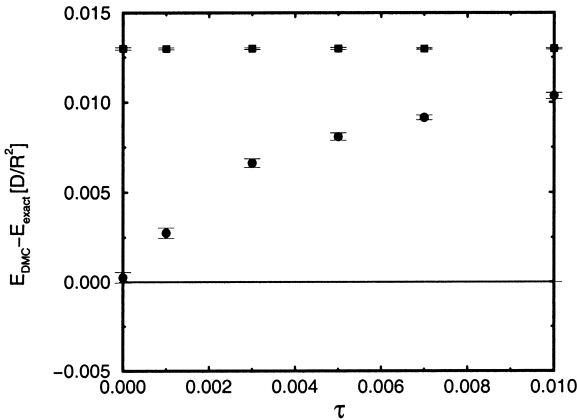


Fig. 5. The difference between the computed and exact excited state energies for the trial state with the exact phase $\psi'_{T1}(\lambda = 1)$ (circles) and the trial state with an approximate phase $\psi'_{T2}(\alpha = 0.0015)$ (squares) for various values of time step. The extrapolated results to time step $\tau = 0$ are also displayed. For the trial state with the exact phase one finds the exact solution and for the trial state with an approximate phase one finds a variational upper bound for the exact solution.

Again, we introduce two trial states

$$\psi'_{T1} = \left(\frac{|z|}{z(1+|z|^2)} \right)^{\mathcal{S}+1} \frac{|z|}{1+\lambda|z|^2}, \quad \psi'_{T2} = \left(\frac{|z|}{z(1+|z|^2)} \right)^{\mathcal{S}+1} |z| \left(\frac{|z|}{z} \right)^\alpha \quad (52)$$

which for $\lambda = 0$ and $\alpha = 0$ each reduce to the exact excited state. As before, for $\lambda \neq 0$ the modulus of ψ'_{T1} is approximate and the phase is exact, and for $\alpha \neq 0$ the modulus of ψ'_{T2} is exact and the phase is approximate.

Figure 5 shows the difference between FP DMC energies computed using trial states $\psi'_{T1}(\lambda = 1)$ and $\psi'_{T2}(\alpha = 0.0015)$ and the exact excited state energy for different values of time step τ as well as the extrapolated $\tau = 0$ result.⁽²³⁾ Again, when the phase of the trial state is exact we obtain the exact energy (circles), $E_1 = (3/2 + 1/\mathcal{S}) \hbar\omega_c$, and when the phase is approximate we obtain a variational upper bound on that energy (squares).

Figure 6 displays the density profiles corresponding to the trial state $\psi'_{T1}(\lambda = 1)$ (VMC), the FP density (FP mixed estimator), the extrapolated density, computed as above by taking the ratio of square of the FP density and the VMC density (Extrap. estimator), and the exact density (Exact). As for the GS, the FP estimator improves on the VMC result, and the extrapolated density is nearly equal to the exact excited state density.

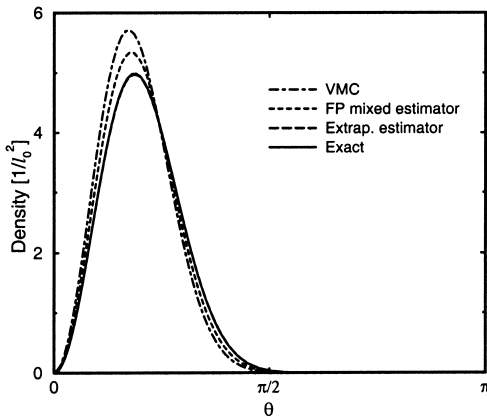


Fig. 6. Excited state density corresponding to the trial state $\psi'_{T1}(\lambda = 1)$ (VMC), FP density with the same state at time step $\tau = 0.001$ (FP mixed estimator), the extrapolated density, which is computed by taking the ratio of square of the FP density and the VMC density (Extrap. estimator), and the exact density (Exact). The FP estimator improves on the VMC result, but still differs from the exact density. The extrapolated density allows one to improve on the FP diffusion Monte Carlo result and is very close to the exact. The density is normalized in such a way that its integral over the surface of the sphere is $4\pi R^2$.

VI. DISCUSSION AND CONCLUSIONS

In this paper we have introduced a stochastic method to solve the many-body Schrödinger equation on curved manifolds. This method is essentially a generalized Diffusion Monte Carlo (DMC) technique allowing one to deal with the effects of space curvature. Such curvature leads to new terms—quantum corrections—in the diffusion matrix and drift vector which appear in the Green's function used as a conditional probability in DMC simulations. Expressions for these corrections for general metric tensors have been worked out in detail.

To illustrate the general methodology we have concentrated on the problem of interacting fermions in external electromagnetic potentials. In this case a variational upper bound to the exact ground state energy can be found by applying the Fixed-Phase approximation, where the fermionic problem is treated as a bosonic one by fixing the phase of the many-body wave function (which is complex-valued in general) by some trial phase. As an example, we have considered the problem of a single electron confined to the surface of a two-sphere, which has a magnetic monopole at its center. This problem can be solved in closed form and, therefore, we have used it as a toy model for testing our technique. In the paper we have presented two calculations, where the ground and first excited state energies are computed using the exact phases, but approximate modulus for the corresponding guiding functions. We have shown that the exact energies are reproduced within statistical accuracy thus proving that the approach for dealing with the quantum corrections is valid.

As emphasized in the Introduction, the method presented in this paper for performing DMC simulations on curved manifolds can be used to study many interesting physical systems. An important example is the quantum Hall (QH) effect, a phenomenon which occurs when a two-dimensional electron system is placed in a strong magnetic field. As first pointed out by Haldane,⁽¹⁹⁾ the electron-monopole system described in Section V provides a convenient geometry for performing finite size numerical studies of QH systems when many interacting electrons are placed on the sphere. This is in part because the spherical geometry has no boundary so that finite size effects are suppressed. In addition, the spherical geometry is conceptually simpler than the (flat metric) torus geometry, which also has no boundary, because on the torus the topological order exhibited by QH states leads to certain nontrivial degeneracies.⁽²⁴⁾

Recently we have used the method developed in this paper to study the fractionally charged quasiparticle excitations of the fractional QH effect,⁽²⁵⁾ and the charged spin texture excitations (skyrmions) of the integer QH effect.⁽²⁶⁾ Previous numerical studies of these excitations have been based on

either VMC or exact diagonalization calculation which, for the most part, have assumed that the wave functions describing the excitations are confined to the lowest ($n = 0$) Landau level. In fact, this is a poor approximation for real experimental systems which can exhibit significant Landau level mixing due to the electron-electron interaction. It has been shown that the FP DMC method provides a systematic way to include the effect of Landau level mixing on QH states,⁽¹⁵⁾ and so the generalization of this method to curved manifolds described in this paper was used in our calculations to perform such studies using Haldane's spherical geometry. Along with the test case of the electron-monopole system, these calculations of Landau level mixing effects in QH systems using the Haldane sphere have shown that the method presented here for performing FP DMC calculations on curved manifolds is a useful tool for studying many interesting physical systems.

ACKNOWLEDGMENTS

We acknowledge stimulating discussions with David Ceperley. V.M. is supported by NSF grant number DMR-9725080. Work at Los Alamos is sponsored by the US DOE under contract W-7405-ENG-36. N.E.B. is supported by US DOE grant number DE-FG02-97ER45639.

REFERENCES

1. D. C. Mattis, *The Many-Body Problem* (World Scientific, Singapore, 1993).
2. For an introduction see, e.g., J. W. Negele and H. Orland, *Quantum Many-Particle Systems* (Addison Wesley, Redwood City, 1988), Ch. 8.
3. D. M. Ceperley, in *Recent Progress in Many-Body Theories*, E. Schachinger, H. Mitter, and M. Sormann, eds. (Plenum, 1995).
4. L. Parker, *Phys. Rev. D* **22**:1922 (1980).
5. C. Yannouleas, E. N. Bogachek, and U. Landman, *Phys. Rev. B* **53**:10225 (1996).
6. Whenever mention is made of a random-walk we mean a Markov chain that is defined as a sequence $\mathcal{R}_1, \mathcal{R}_2, \dots, \mathcal{R}_K$ of K random variables that take values in configuration space, i.e., the space of particle positions. As usual, what characterizes a random-walk is its initial probability distribution and a conditional probability that dictates the transition from \mathcal{R}_i to \mathcal{R}_{i+1} . This transition probability is non-unique and discretization dependent.⁽⁸⁾ Among all the possible choices we will require a prepoint discretization of the transition probability (short-time propagator) because we will use Monte Carlo methods to generate the walkers.
7. G. B. Bachelet, D. M. Ceperley, and M. G. B. Chiochetti, *Phys. Rev. Lett.* **62**:2088 (1989).
8. F. Langouche, D. Roekaerts, and E. Tirapegui, *Il Nuovo Cimento* **53 B**:135 (1979).
9. L. D. Landau and E. M. Lifshitz, *The Classical Theory of Fields* (Butterworth-Heinemann, Oxford, 1999), Ch. 10.

10. The effects of an external magnetic field on a system of electrons can be profound. The field couples to the electron's charge and spin, modifying its spatial motion and lifting its spin degeneracies. The field can also create spatial anisotropy, effectively reducing the dimensionality of the system from three to two. The combination of the reduced dimensionality, strong particle interactions and the field itself is known to have novel consequences, like the formation of isotropic fractional QH fluids, which are incompressible states of the two-dimensional homogeneous Coulomb gas.
11. \mathcal{M}^N is the Cartesian product manifold of dimension dN .
12. M. Hamermesh, *Group Theory* (Addison Wesley, Reading, 1962).
13. Remember that in a general metric space the resolution of the identity operator with respect to the spectral family of the position operator is $\mathbb{1} = \int_{\mathcal{M}^N} \omega |\mathcal{R}\rangle\langle\mathcal{R}|$.
14. The main difficulty is to define a probability measure (semi-positive definite) which allows one to get the complex-valued state with no asymptotic signal-to-noise ratio decay in Euclidean time ("phase problem"⁽¹⁵⁾). This translates into a problem of geometric complexity, which is solved approximately using constraints in the manifold where the wave function has its support. In this way, we get stable but approximate solutions which can be systematically improved.
15. G. Ortiz, D. M. Ceperley, and R. M. Martin, *Phys. Rev. Lett.* **71**:2777 (1993).
16. For a discussion of quantum corrections see, for example, B. S. DeWitt, *Rev. Mod. Phys.* **29**:377 (1957); and D. W. McLaughlin and L. S. Schulman, *J. Math. Phys.* **12**:2520 (1971).
17. A. M. Polyakov, *Gauge Fields and Strings* (Harwood, Chur, 1993), p. 176.
18. P. J. Reynolds, D. M. Ceperley, B. J. Alder, and W. A. Lester, Jr., *J. Chem. Phys.* **77**:5593 (1982).
19. F. D. M. Haldane, *Phys. Rev. Lett.* **51**:605 (1983).
20. T. T. Wu and C. N. Yang, *Nucl. Phys. B* **107**:365 (1976).
21. For real symmetric Hamiltonians, this catastrophe is known as the "fermion-sign" problem. For a recent study, see M. H. Kalos and K. E. Schmidt, *J. Stat. Phys.* **89**:425 (1997).
22. For trial state ψ_{T1} we used $\lambda = 1$, the number of walkers was chosen to be $N_w = 300$, the number of Monte Carlo steps per walker was 2×10^7 , and the acceptance rate was between 97% and 99.5%. For trial state ψ_{T2} we used $\alpha = 0.001$, the number of walkers was $N_w = 100$, the total number of Monte Carlo steps per walker was 10^6 , and the acceptance rate was the same as for ψ_{T1} .
23. The parameters (number of walkers, number of Monte Carlo steps, etc.) used for these simulations were the same as those used for the ground state simulations except that we took $\alpha = 0.0015$ in ψ'_{T2} .
24. F. D. M. Haldane, *Phys. Rev. Lett.* **61**:1029 (1988).
25. V. Melik-Alaverdian, N. E. Bonesteel, and G. Ortiz, *Phys. Rev. Lett.* **79**:5286 (1997).
26. V. Melik-Alaverdian, N. E. Bonesteel, and G. Ortiz, *Phys. Rev. B* **60**:R8501 (1999).